JOINT INSTITUTE FOR ADVANCEMENT OF FLIGHT SCIENCES

Program of Research in Laminar Flow Control in the JIAFS at NASA Langley Research Center

(NASA-CR-164843) PROGRAM OF RESEARCH IN LAMINAR FLOW CONTROL IN THE JIAFS AT NASA LANGLEY RESEARCH CENTER Status Report, 1 Jan. - 30 Jun. 1981 (George Washington Univ.) 15 p HC A02/MF A01 CSCL 01C G3/02

N81-32121

Unclas 37500

NASA Grant NSG 1585

Status Report
January 1, 1981 to June 30, 1981

School of Engineering and Applied Science
The George Washington University
Washington, DC 20052

STATUS REPORT FOR GEORGE WASHINGTON UNIVERSITY

W. Pfenninger, July 1981

Some Thoughts About all Laminar Flow High Subsonic Speed LFC Airplanes

With the laminar surface friction being five to ten times lower than the turbulent friction drag at high length Reynolds numbers, the performance of a low drag suction LFC airplane is essentially controlled by the induced drag and the turbulent friction drag of the nonlaminarized area. The question then arises as to how the airplane cruise lift to drag ratio $(\frac{L}{D})_{cruise}$ increases with increasing extent of laminar flow $0_{lam.}/0_{total}$ (0 = airplane wetted area). In particular, the question arises as to the airplane performance in the optimum case with all laminar flow over the airplane wetted area. The question then further arises concerning design approaches of all laminar flow LFC airplanes which optimize the airplane range $R=\eta_{OV} \cdot (\frac{L}{D}) \cdot H \cdot \ln(W_O/W_E)$.

The following simplified analysis assumes that $C_{D_O} = C_{D_\infty} + C_{D_{parasite}}$ is independent of Reynolds number and C_L. A linear variation of C_{D_O} with $0_{lam.}/0_{total}$ is assumed: $C_{D_O} = C_{D_{O_{all\ turb.}}} - 0.01. \frac{0_{lam.}}{0_{total}}$, where $C_{D_{O_{all\ turb.}}} = 0.012$ and $C_{D_{O_{all\ laminar}}} = 0.002.$ (*)

(*) $C_{D_{\infty_{wing}}} = .0010$ (including equivalent suction drag),

$C_{D_{parasite}} = .0010.$

The optimum airplane cruise lift to drag ratio is then $(\frac{L}{D})_{opt} = \sqrt{\frac{\pi}{4} \cdot \frac{b^2/S}{C_{D_O}}}$. The corresponding $C_{L_{opt}}$ is $C_{L_{opt}} = \sqrt{\pi \cdot \frac{b^2}{S} \cdot C_{D_O}}$.

The corresponding average wing chord Reynolds number $Re_{\bar{c}}$ is proportional to $\frac{1}{M \cdot C_L} \sqrt{W} \cdot \sqrt{\frac{W/S}{b^2/S}}$ or $\frac{1}{MC_L} \sqrt{W} \sqrt{\frac{W}{b^2}}$. The figures 1-3 show plots of $(\frac{L}{D})_{opt}$, $C_{L_{opt}}$, $Re_{\bar{c}}$ versus the ratio $(\frac{O_{lam.}}{O_{total}})$ (laminar to total airplane wetted area O) for different wing aspect ratios b^2/S. With increasing laminarization of the airplane wetted areas $(\frac{L}{D})_{opt}$ increases first relatively slowly and rises progressively rapidly to phenomenally high values as full laminarization is approached, especially for high wing aspect ratios b^2/S (fig. 1). While at lower ratios $(\frac{O_{lam.}}{O_{total}})$ the value of the laminar surface friction is relatively unimportant, it critically affects $(\frac{L}{D})_{cruise}$ in the case of extensive or complete airplane laminarization (fig. 4). In other words, while it is unimportant to fight for particularly low laminar surface friction values up to moderately large $(\frac{O_{lam.}}{O_{total}})$ - ratios, it becomes critically important to minimize the laminar surface friction in the case of extensive or complete airplane laminarization.

According to fig. 2 $C_{L_{opt}}$ decreases substantially with increasing $(\frac{O_{lam.}}{O_{total}})$ - ratios to surprisingly low values for extensive or complete airplane laminarization. $C_{L_{opt}}$ increases proportional to $\sqrt{b^2/S}$. At very high (b^2/S) - values $C_{L_{opt}}$ becomes eventually impractically high for airplanes with extensive turbulent flow from the standpoint of a high critical Mach number and a satisfactory rear pressure recovery on the upper wing surface. Thus, the advantage of a high aspect ratio wing cannot be fully exploited for airplanes with extensive turbulent flow without a severe penalty in design cruise speed. On the other hand, with extensive or complete airplane laminarization $C_{L_{opt}}$ decreases to rather low $C_{L_{opt}}$ - values, especially for smaller wing aspect ratios b^2/S, such that the resulting high cruise flight dynamic pressures lead to increased wing strucutral weights. Therefore, to avoid unduly low $C_{L_{opt}}$ - values for extensive or complete airplane laminarization, all laminar LFC airplanes should preferably be laid out for higher wing aspect ratios, larger spans and lower span loadings (W/b^2). The problem of designing such large span high aspect ratio wings for all laminar flow airplanes is then reduced to the minimization of the structural weight for such long LFC wings with satisfactory structural strength, stiffness and fatigue characteristics.

The relatively low $C_{L_{opt}}$ - values of all laminar LFC airplanes, of course, are advantageous from the standpoint of a high airplane design Mach number. Vice versa, for a given M_{Design}, the wing thickness ratio t/c could be increased to either save wing structural weight or to increase wing span for induced drag reduction. Alternatively, wing sweep might be reduced substantially to minimize boundary layer crossflow - and front wing attachment line flow problems as well as flyspeck - and ice crystal contamination problems in ice clouds, provided wing gust loads at such low sweep angles can be alleviated by means of active control. From the standpoint of buffeting and drag rise, wings with an excessively large thickness ratio t/c are undesirable; therefore, wing sweep angles should be considered which lead to moderately high wing thickness ratios. If it should prove possible to maximize the airfoil design Mach number $M_{\infty_{Design}}$ by suitable means as discussed in ref. 1, the required wing sweep angle for a $M_{cruise} = 0.80$ airplane becomes surprisingly small, as shown in fig. 5 for different $(t/c)_{ratios}$ and C_L - values. (For airfoil X63 T18 K = .9460). With such small sweep angles swept forward wings become attractive, atleast in advanced composite structure when wing divergence can be avoided at but a minor weight penalty by suitable orientation of the spanwise composite plies. Wing divergence can be further controlled by an active horizontal control surface located on a boom downstream of a fuel- or payload nacelle placed in the outer wing. Active control of the wing loads by means of a small chord trailing edge cruise flap will further alleviate the divergence problems of swept forward wings.

A large span high aspect ratio wing of low structural weight appears possible by bracing the wing externally for wing bending - as well as torsional loads by means of suction laminarized wide chord struts. The small wing bending moments in the braced inboard wing area enable thin wings of low profile drag and a high wing drag divergence - and buffet Mach number to render the whole airplane less sensitive to high speed buffeting. Swept forward LFC wings are inherently advantageous for all laminar

LFC airplanes:

1) The leading edge sweep of a tapered swept forward LFC wing is smaller than the average wing sweep to further alleviate the leading edge boundary layer crossflow - and front attachment line flow problems as well as leading edge flyspeck - and ice crystal contamination and LFC maintenance problems.

2) With the wing isobar sweep on a tapered swept forward wing increasing in chordwise direction $c_p{}^*$ (for $M_\perp = 1$ normal to the isobars) decreases from the leading- to the trailing edge to induce an additional chordwise flow acceleration, favorable for laminarization in the region of the flat pressure distribution.

3) With a large span externally braced high aspect ratio swept forward wing a larger percentage of the fuselage can be arranged upstream of the wing-fuselage intersection to enable laminarization over a large percentage of the body length, especially if a fuselage with a relatively low length to diameter ratio is acceptable at $M_{cruise} = .80$. The tail surfaces would then be supported by suction laminarized struts of very low parasite drag (fig. 7). The parasite drag of the fuselage and empennage system could then be extremely low to maximize $(L/D)_{cruise}$.

Fig. 3 shows the variation of $Re_{\bar{c}}$ with $\frac{0_{lam.}}{0_{total}}$ for different b^2/S - values. For a given b^2/S - value $Re_{\bar{c}}$ increases (due to the lower $C_{L_{opt}}$ and the corresponding lower optimum cruise altitude). However, as the wing aspect ratio increases $Re_{\bar{c}}$ decreases inversely proportional to b^2/S to alleviate accordingly the suction laminarization problems. A more detailed study which considers the variation of $C_{D_{laminar}}$ with Reynolds number shows somewhat lower

$C_{L_{opt}}$ - values than for the case of constant $C_{D_{laminar}}$ with $Re_{\bar{c}}$ (fig. 6). Even with a wing aspect ratio as high as 30, $C_{L_{opt}}$ for $(L/D)_{opt} = 110$ is as low as .35 ($M = .80$) for an all laminar flow LFC airplane of $W_O = 133000$ kg take off gross weight. The corresponding wing chord - and unit length Reynolds numbers $Re_{\bar{c}}$ and $\frac{U_\infty}{V}$ are relatively small. Fig. 7 shows a possible layout of such a practically all laminar flow turboprop powered low drag suction prototype airplane cruising at $M_\infty = .80$. With the propeller operating in the decelerated rear flow field of the fuselage, the axial local flow Mach number at the propeller tip is 0.76 at a flight Mach number 0.80 to alleviate accordingly the propeller design problems due to compressibility. The suction laminarized wing struts upstream of the propeller can be used as inlet guide vanes, thus recovering a large part of the substantial propeller rotational slip stream energy, raising the propeller cruise efficiency at M = 0.80 close to 0.90. Combined with the extremely high cruise lift to drag ratio $(\frac{L}{D}) \doteq 100$ and a low structural weight, possible by the strutbraced design of the advanced composite wing, the wing load alleviation both in bending and torsion(*) by the outboard suction laminarized nacelle with its active control surface, as well as by the trailing edge cruise flap, etc., an unprecedented all-out range beyond all previous expectations appears possible

(*)Wing torsional deformation could be actively controlled by the above mentioned horizontal control surfaces located in the rear part of these nacelles, activated by inertial platforms in the fuselage and the nacelles such that the wing angle of attack at the location of the nacelles remains the same as at the fuselage wing intersection.

($\geq$ 200000 kilometers). LFC research needed in connection with the development of such a prototype LFC airplane of 133000 kg take-off gross weight would be primarily concerned with the verification of suction laminarization in the transonic flow region particularly of the upper wing surface and the verification of the stabilizing influence of a relatively rapid flow turning over short chordwise distances in the concave areas of the front and rear lower surface. Boundary layer cross-flow would not be a problem, i.e. straight wing LFC experiments at relatively low $Re_{\bar{c}}$'s appear adequate for these research investigations.

References:

1. W. Pfenninger and J. K. Viken; Supercritical LFC Airfoils for all Laminar Flow $M_\infty = 0.80$ LFC Airplanes; GWU Summary Report; July 1981.

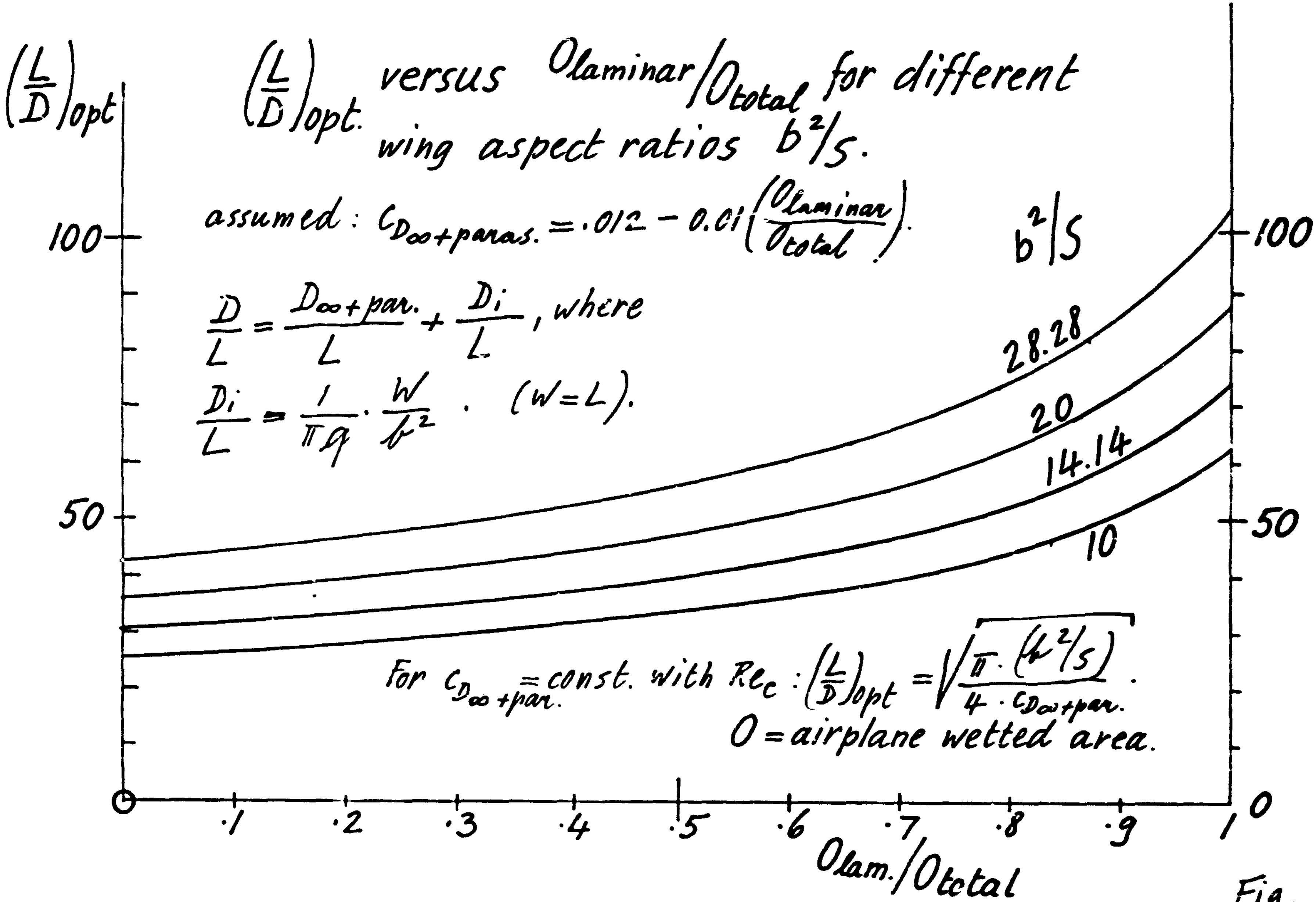

$\left(\frac{L}{D}\right)_{opt}$
$\left(\frac{L}{D}\right)_{opt.}$ versus $O_{laminar}/O_{total}$ for different wing aspect ratios b^2/S.
assumed: $c_{D_{\infty+paras.}} = .012 - 0.01\left(\frac{O_{laminar}}{O_{total}}\right)$.
$\frac{D}{L} = \frac{D_{\infty+par.}}{L} + \frac{D_i}{L}$, where
$\frac{D_i}{L} = \frac{1}{\pi q} \cdot \frac{W}{b^2}$. $(W=L)$.
For $c_{D_{\infty+par.}}$ = const. with Re_c : $\left(\frac{L}{D}\right)_{opt} = \sqrt{\frac{\pi \cdot (b^2/S)}{4 \cdot c_{D_{\infty+par.}}}}$.
O = airplane wetted area.
b^2/S
28.28
20
14.14
10
100
50
0
·1
·2
·3
·4
·5
·6
·7
·8
·9
1
$O_{lam.}/O_{total}$

Fig. 1

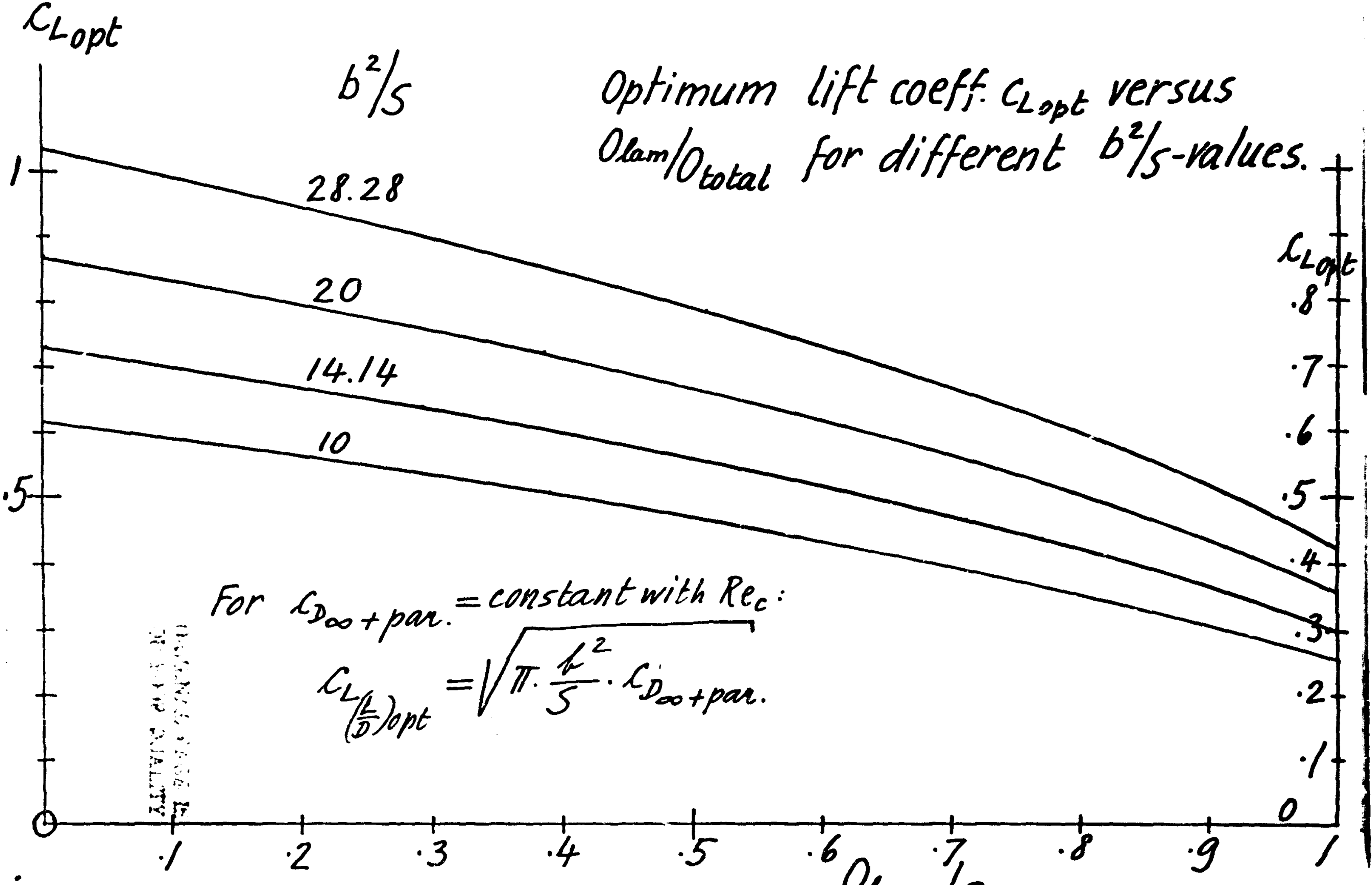

Optimum lift coeff. $c_{L_{opt}}$ versus O_{lam}/O_{total} for different b^2/S-values.
$c_{L_{opt}}$
b^2/S
28.28
20
14.14
10
For $c_{D_{\infty}+par.}$ = constant with Re_c:
$c_{L_{(L/D)opt}} = \sqrt{\pi \cdot \frac{b^2}{S} \cdot c_{D_{\infty}+par.}}$
$O_{lam.}/O_{total}$
0
·1
·2
·3
·4
·5
·6
·7
·8
·9
1

Fig. 2

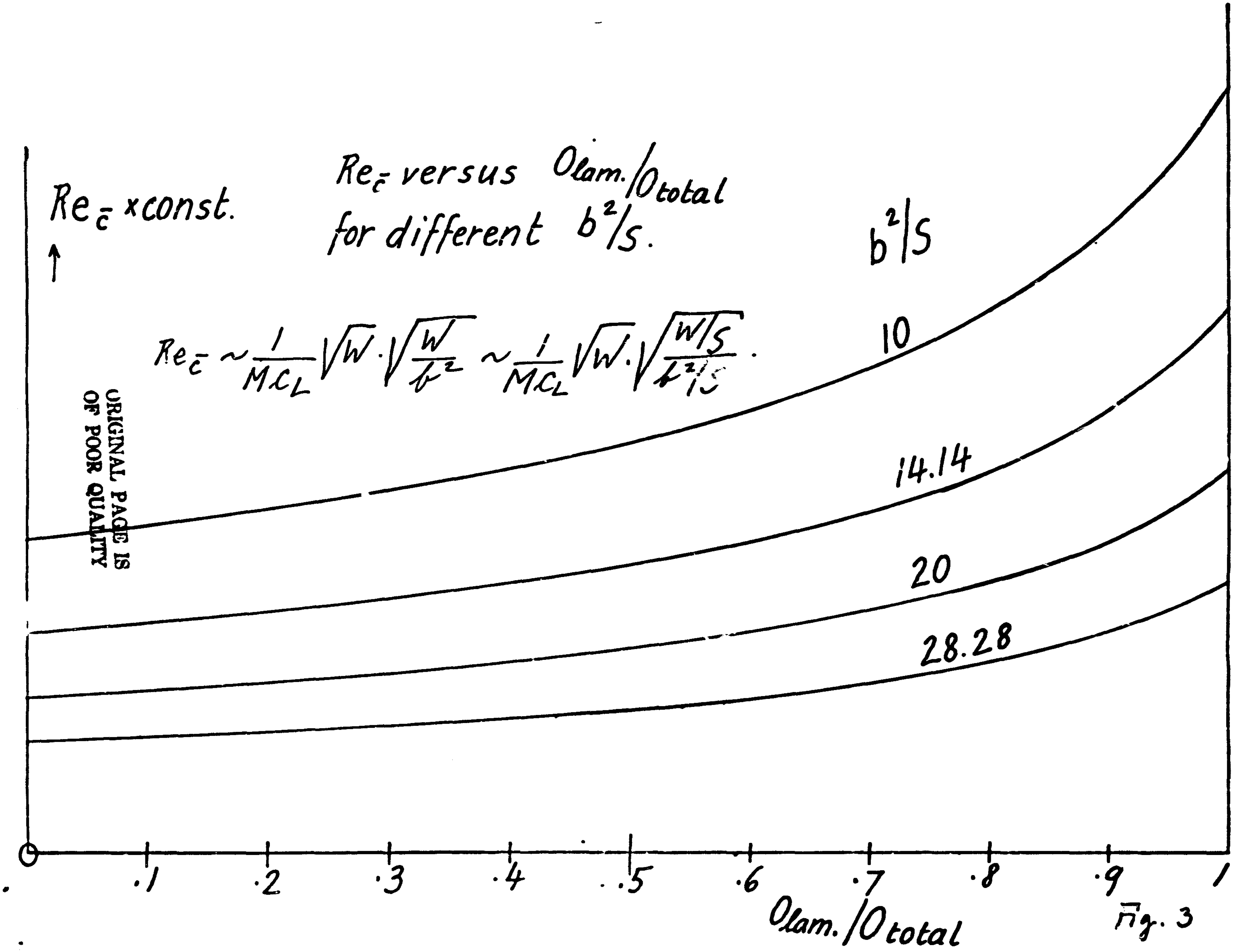

$Re_{\bar{c}} \times$ const.
$Re_{\bar{c}}$ versus $O_{lam.}/O_{total}$
for different b^2/S.
b^2/S
10
14.14
20
28.28
$Re_{\bar{c}} \sim \frac{1}{MC_L}\sqrt{W}\cdot\sqrt{\frac{W}{b^2}} \sim \frac{1}{MC_L}\sqrt{W}\cdot\sqrt{\frac{W/S}{b^2/S}}$.
0
.1
.2
.3
.4
.5
.6
.7
.8
.9
1
$O_{lam.}/O_{total}$

Fig. 3

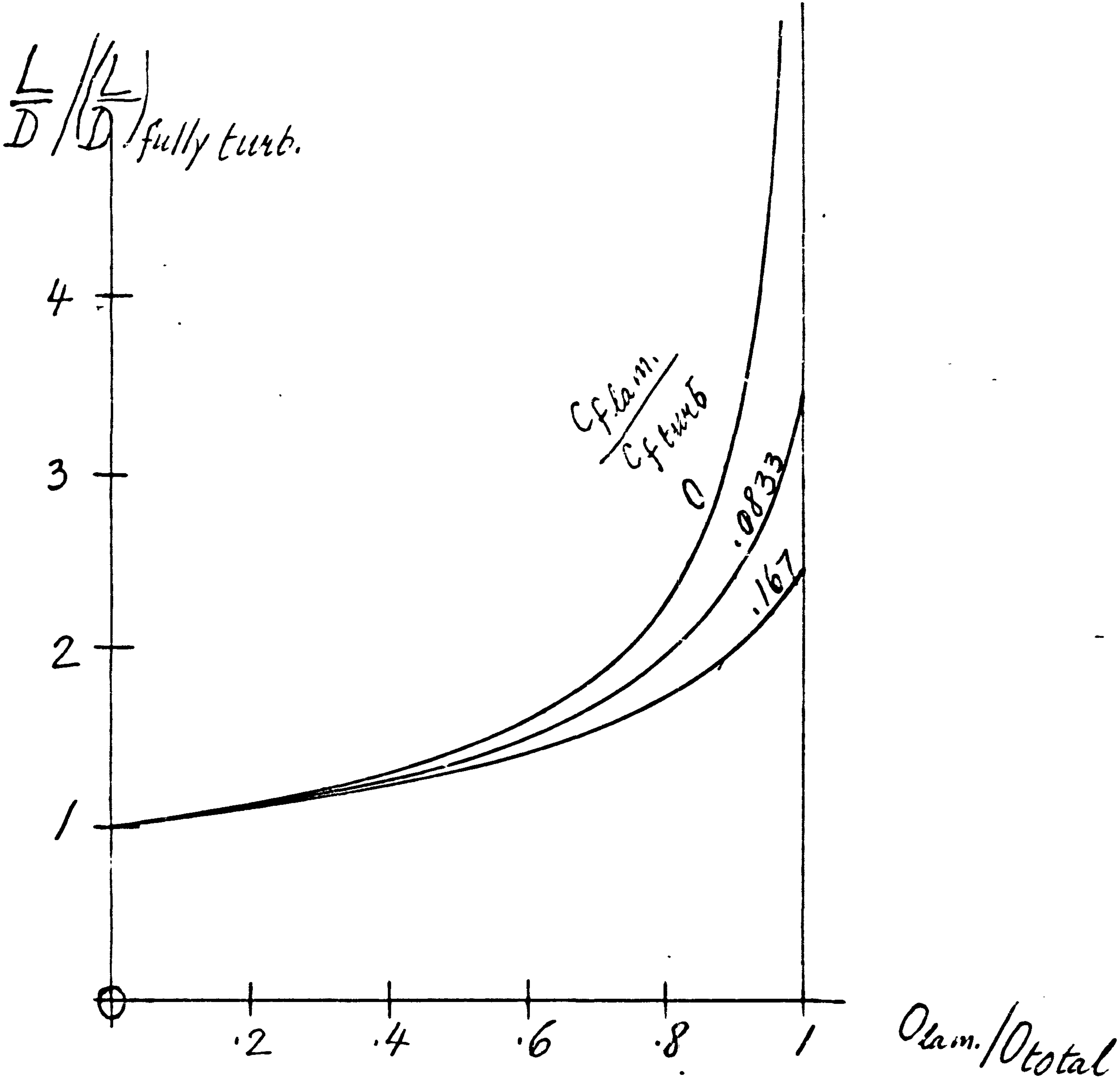
L/D / (L/D) fully turb.
4
3
2
1
0
Cf lam. / Cf turb
0
.0833
.167
·2
·4
·6
·8
1
θlam. / θtotal

Fig. 4

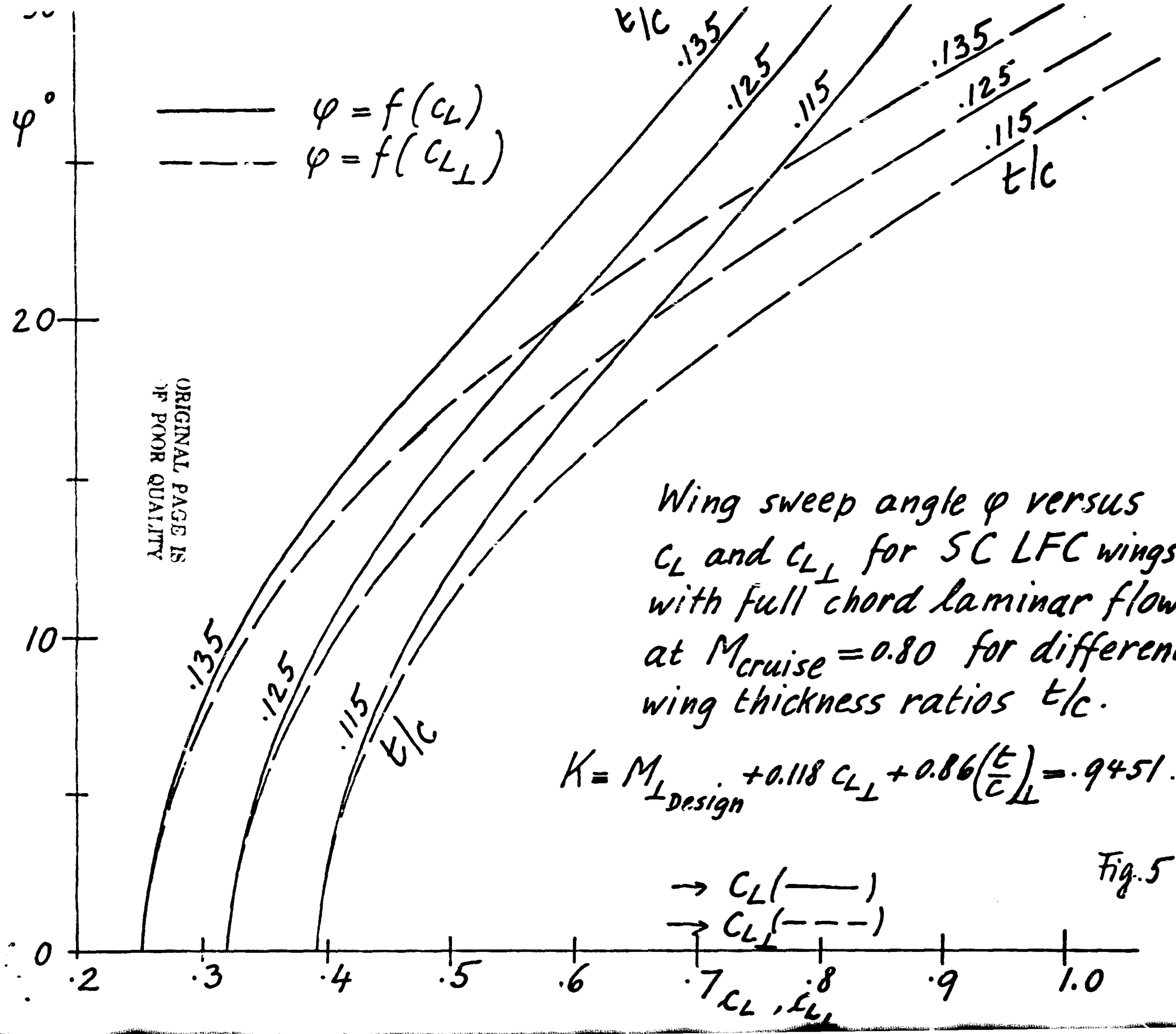

Wing sweep angle φ versus C_L and $C_{L_\perp}$ for SC LFC wings with full chord laminar flow at $M_{cruise} = 0.80$ for different wing thickness ratios t/c.

$$K = M_{\perp Design} + 0.118\, C_{L_\perp} + 0.86\left(\frac{t}{c}\right)_\perp = .9451.$$

Fig. 5

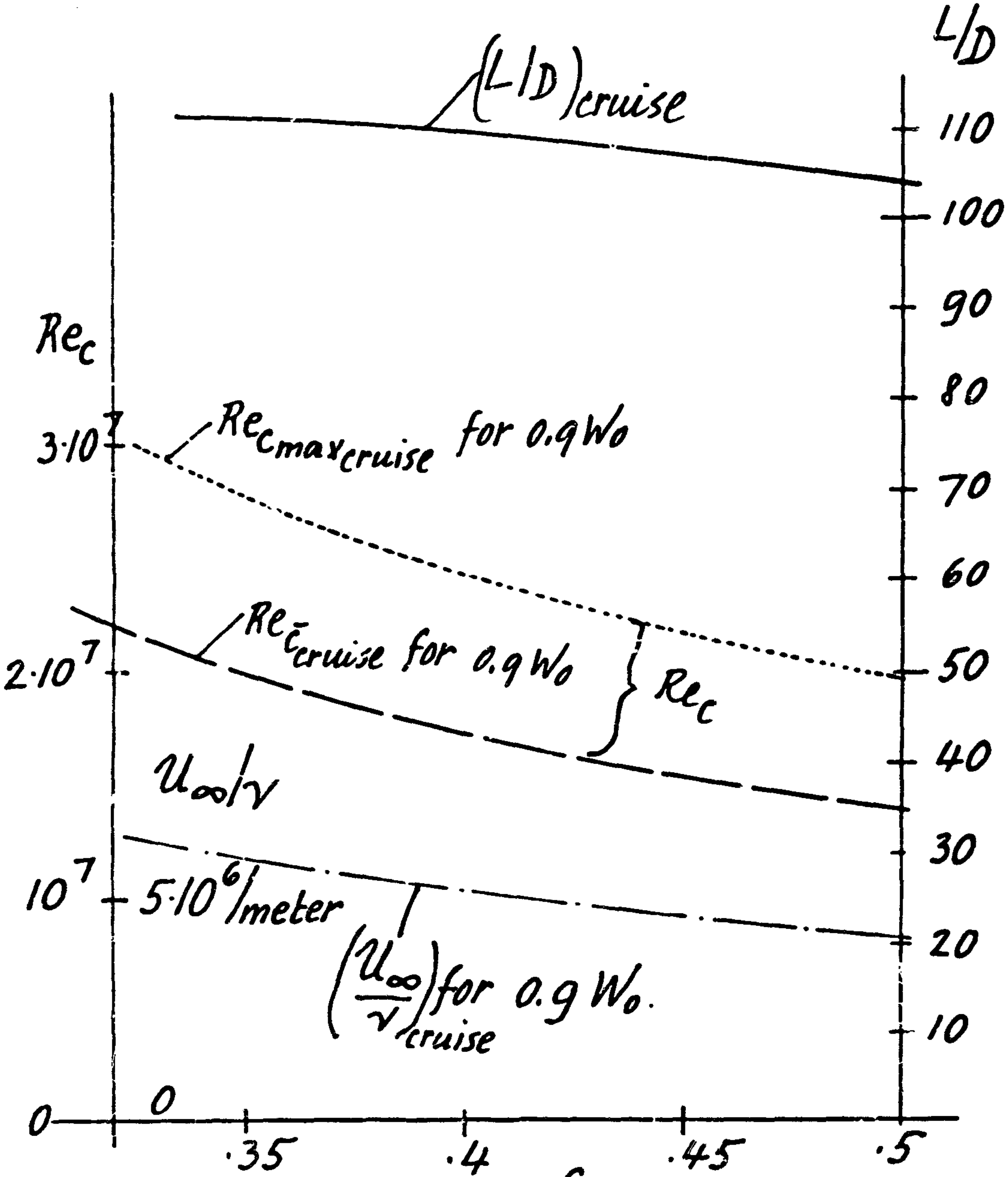

Fig. 6

All laminar $M = .8$ LFC airplane, $\frac{b^2}{S} = 30$, $W_0 = 133000\,kg$

$C_{D\infty} + par. \cong .002$ at $C_L = .4$; $W_0/S = 400\ kg/m^2$.

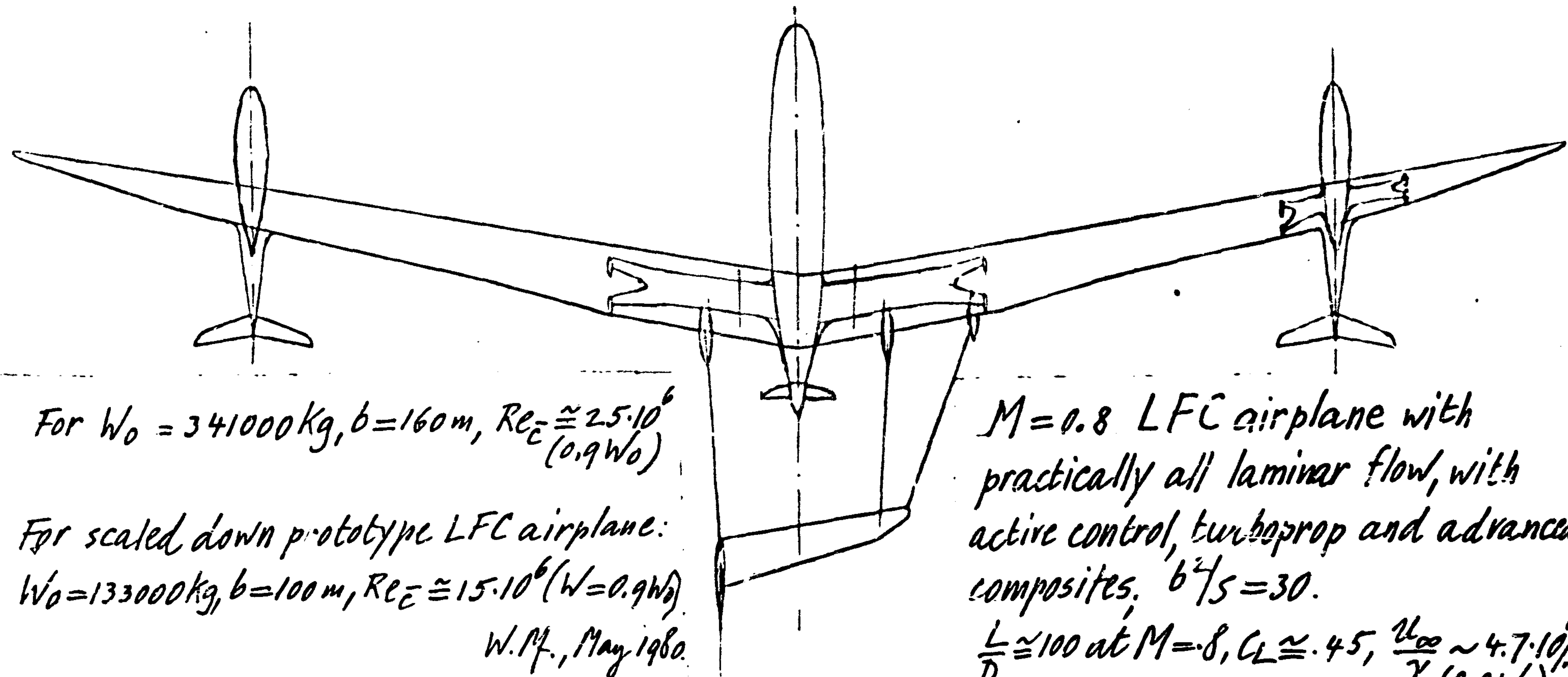

For $W_0 = 341000\,Kg$, $b = 160\,m$, $Re_{\bar{c}} \cong 25 \cdot 10^6$ $(0.9W_0)$

For scaled down prototype LFC airplane:
$W_0 = 133000\,kg$, $b = 100\,m$, $Re_{\bar{c}} \cong 15 \cdot 10^6$ $(W = 0.9W_0)$

W.Pf., May 1980

$M = 0.8$ LFC airplane with practically all laminar flow, with active control, turboprop and advanced composites. $b^2/S = 30$.
$\frac{L}{D} \cong 100$ at $M = .8$, $C_L \cong .45$, $\frac{u_\infty}{\nu} \sim 4.7 \cdot 10^6/m$ $(0.9W_0)$

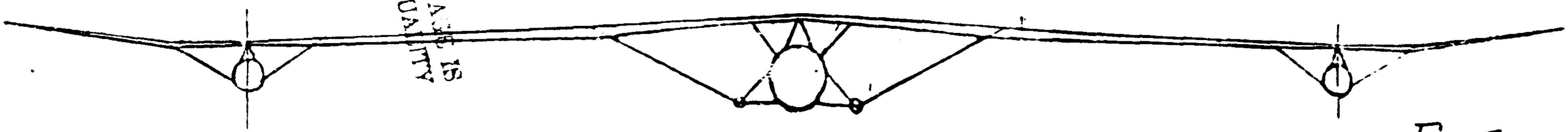

Fig. 7